



HAL
open science

Multi-dimensional Optimal Order Detection (MOOD) - A very high-order Finite Volume Scheme for conservation laws on unstructured meshes.

Steven Diot, Stéphane Clain, Raphaël Loubère

► **To cite this version:**

Steven Diot, Stéphane Clain, Raphaël Loubère. Multi-dimensional Optimal Order Detection (MOOD) - A very high-order Finite Volume Scheme for conservation laws on unstructured meshes.. 2011. hal-00566023

HAL Id: hal-00566023

<https://hal.science/hal-00566023>

Preprint submitted on 15 Feb 2011

HAL is a multi-disciplinary open access archive for the deposit and dissemination of scientific research documents, whether they are published or not. The documents may come from teaching and research institutions in France or abroad, or from public or private research centers.

L'archive ouverte pluridisciplinaire **HAL**, est destinée au dépôt et à la diffusion de documents scientifiques de niveau recherche, publiés ou non, émanant des établissements d'enseignement et de recherche français ou étrangers, des laboratoires publics ou privés.

Multi-dimensional Optimal Order Detection (MOOD) — A very high-order Finite Volume Scheme for conservation laws on unstructured meshes

S. Clain, S. Diot, and R. Loubère

Abstract The Multi-dimensional Optimal Order Detection (MOOD) method is an original Very High-Order Finite Volume (FV) method for conservation laws on unstructured meshes. The method is based on an *a posteriori* degree reduction of local polynomial reconstructions on cells where prescribed stability conditions are not fulfilled. Numerical experiments on advection and Euler equations problems are drawn to prove the efficiency and competitiveness of the MOOD method.

Key words: MOOD, high-order, finite volume, unstructured meshes, limitation, Euler equations, conservation laws

1 Introduction

The Multi-dimensional Optimal Order Detection has been introduced in [5] as an original High-Order Finite Volume method for conservation laws on unstructured meshes. As multi-dimensional MUSCL [3, 2, 7, 4] or ENO/WENO methods [1, 6, 9], the MOOD method is based on a high-order space discretization with local polynomial reconstructions coupled with a high-order TVD Runge-Kutta method for time discretization.

The main difference between classical high-order methods and the MOOD one is that the limitation procedure is done *a posteriori*. Inside a time step,

S. Clain

Departamento de Matemática e Aplicações, Campus de Gualtar - 4710-057 Braga
Campus de Azurm - 4800-058 Guimares, Portugal, e-mail: clain@math.uminho.pt

S. Diot, R. Loubère

Institut de Mathématiques de Toulouse, Université de Toulouse, France, e-mail:
steven.diot@math.univ-toulouse.fr, raphael.loubere@math.univ-toulouse.fr

a first solution is computed with numerical fluxes evaluated from unlimited high-order polynomial reconstructions. Then polynomial degrees are reduced on cells where prescribed stability conditions are not fulfilled and the solution is re-evaluated. That iterative procedure provides a solution which respects the stability constraints.

The present article is devoted to an extension of the MOOD method to a sixth-order space discretization on triangular meshes. Numerical tests for the advection problem and Euler equations with gravity are given in last section.

2 Framework

We consider the scalar hyperbolic equation defined on a bounded polygonal domain $\Omega \subset \mathbb{R}^2$ written in its conservative form

$$\begin{aligned} \partial_t u + \nabla \cdot F(u) &= 0, \\ u(\cdot, 0) &= u_0, \end{aligned} \quad (1)$$

where $u = u(\mathbf{x}, t)$ is the unknown function with $t > 0$, $\mathbf{x} \in \Omega$, F is the physical flux and u_0 stands for the initial condition. We consider a triangular tessellation of Ω where K_i is a generic triangle with centroid \mathbf{c}_i . Moreover \mathbf{n}_{ij} is the unit normal vector of edge e_{ij} from K_i to K_j and q_{ij}^r , $r = 1, 2, 3$, are the gaussian quadrature points of e_{ij} . Finally $\underline{\nu}(i)$ (resp. $\overline{\nu}(i)$) is the index set of cells which share an edge (resp. an edge or a node with K_i). This notation is summarized in Fig. 1.

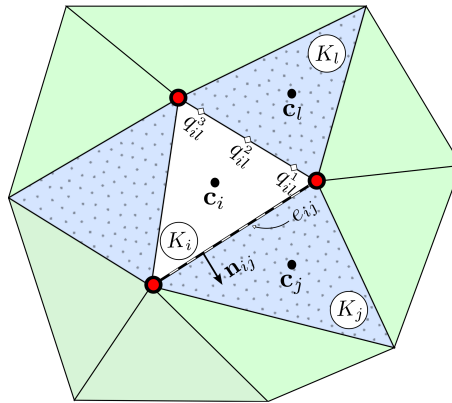


Fig. 1 Mesh notation. Index set $\underline{\nu}(i)$ corresponds to blue cells with dots and $\overline{\nu}(i)$ corresponds to every non-white cells.

We recall the generic first-order Finite Volume discretization of (1)

$$u_i^{n+1} = u_i^n - \Delta t \sum_{j \in \mathcal{L}(i)} \frac{|e_{ij}|}{|K_i|} G(u_i^n, u_j^n, \mathbf{n}_{ij}), \quad (2)$$

where u_i^n is an approximation of the mean value of u on cell K_i at time t^n and $|e_{ij}|$, $|K_i|$ stand for the edge length and the cell surface respectively. We assume that the numerical flux $G(u_i^n, u_j^n, \mathbf{n}_{ij})$ satisfies the consistency and monotonicity properties such that, under an adequate CFL condition, the following Discrete Maximum Principle (DMP) is fulfilled

$$\min_{j \in \mathcal{P}(i)} (u_i^n, u_j^n) \leq u_i^{n+1} \leq \max_{j \in \mathcal{P}(i)} (u_i^n, u_j^n). \quad (3)$$

Only few modifications of (2) are needed to get the following High-Order Finite Volume scheme

$$u_i^{n+1} = u_i^n - \Delta t \sum_{j \in \mathcal{L}(i)} \frac{|e_{ij}|}{|K_i|} \sum_{r=1}^3 \xi_r G(u_{ij,r}^n, u_{ji,r}^n, \mathbf{n}_{ij}), \quad (4)$$

namely the use of a sixth-order gaussian quadrature rule with weights ξ_r ($r = 1, 2, 3$) and the replacement of u_i^n (resp. u_j^n) by $u_{ij,r}^n$ (resp. $u_{ji,r}^n$) which is an approximation of $u(q_{ij}^r, t^n)$ from the high-order polynomial reconstruction on K_i (resp. K_j). Notice that the high-order scheme (4) corresponds to a convex combination of the first-order one (2), that is important from a practical point of view for an easy and effective implementation.

It is well known that methods based on high-order reconstructions without limiting procedure produce spurious oscillations in the vicinity of discontinuities. In order to prevent such oscillations, the today's effective high-order methods (MUSCL, WENO...) use *a priori* limitation procedures. The Multi-dimensional Optimal Order Detection (MOOD) method breaks away from this approach through an original effective iterative procedure based on an *a posteriori* detection of such unphysical oscillations (see Fig. 2). The details of MOOD method are recalled in next section

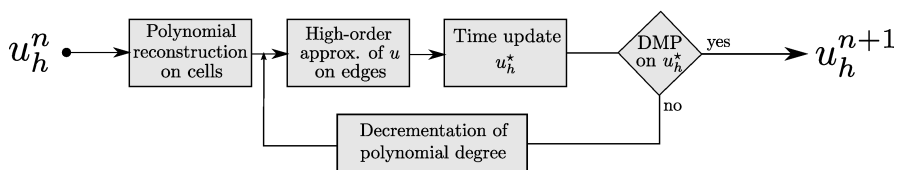


Fig. 2 A simplistic view of the Multi-dimensional Optimal Order Detection concept.

3 MOOD method

For the sake of clarity, we only consider a forward Euler method and one quadrature point per edge. Consequently we denote by u_{ij} (resp. u_{ji}) the high-order approximation of u on edge e_{ij} from cell K_i (resp. K_j).

3.1 Basics

Polynomial reconstruction.

High-order approximations of the solution at quadrature points are mandatory. To this end, multi-dimensional polynomial reconstructions from mean values are carried out. The reader should refer to [6, 5] for detailed presentation of such a technique. However the reconstructed polynomial of arbitrary high-order $d_{max} + 1$ has the form

$$\tilde{u}(x, y) = \bar{u} + \sum_{1 \leq \alpha + \beta \leq d_{max}} \mathcal{R}_{\alpha\beta} \left((x - c_x)^\alpha (y - c_y)^\beta - \frac{1}{|K|} \int_K (x - c_x)^\alpha (y - c_y)^\beta dx dy \right),$$

where (c_x, c_y) is the centroid of a generic cell K and $\mathcal{R}_{\alpha\beta}$ are the unknowns polynomial coefficients.

In this way mean value on K is conserved and the truncation of all terms of degree $\alpha + \beta > \bar{d}$ produces a relevant approximation of u as a polynomial of degree $\bar{d} \leq d_{max}$.

CellPD and EdgePD.

We recall the fundamental notions introduced in [5].

- d_i is the Cell Polynomial Degree (**CellPD**) which represents the degree of the polynomial reconstruction on cell K_i .
- d_{ij} and d_{ji} are the Edge Polynomial Degrees (**EdgePD**) which correspond to the effective degrees used to respectively build u_{ij} and u_{ji} on both sides of edge e_{ij} .

We now detail the MOOD method using both notions in the case of the scalar problem (1).

3.2 Algorithm for the scalar case.

The MOOD method consists of the following iterative procedure which details the concept depicted in Fig. 2.

-
1. **CellPD initialization.** Each CellPD is initialized with \mathbf{d}_{max} .
 2. **EdgePD evaluation.** Each EdgePD is set up as the minimum of the two neighboring CellPD.
 3. **Quadrature points evaluation.** Each u_{ij} is evaluated with the polynomial reconstruction of degree \mathbf{d}_{ij} .
 4. **Mean values update.** The updated values u_h^* are computed using the finite volume scheme (4).
 5. **DMP test.** The DMP criterion is checked on each cell K_i

$$\min_{j \in \overline{\mathcal{P}}(i)} (u_i^n, u_j^n) \leq u_i^* \leq \max_{j \in \overline{\mathcal{P}}(i)} (u_i^n, u_j^n). \quad (5)$$

- If u_i^* does not satisfy (5) the CellPD is decremented, $\mathbf{d}_i := \max(0, \mathbf{d}_i - 1)$.
6. **Stopping criterion.** If all cells satisfy the DMP property, the iterative procedure stops with $u_h^{n+1} = u_h^*$ else go to Step 2.
-

Since only problematic cells and their neighbors in the compact stencil $\underline{\mathcal{P}}(i)$ have to be checked and reupdated during the iterative MOOD procedure, the computational cost is dramatically reduced.

3.3 Algorithm for the Euler equations case.

We now extend the MOOD method to the Euler system, namely

$$\partial_t \begin{pmatrix} \rho \\ \rho u \\ \rho v \\ E \end{pmatrix} + \partial_x \begin{pmatrix} \rho u \\ \rho u^2 + p \\ \rho uv \\ u(E + p) \end{pmatrix} + \partial_y \begin{pmatrix} \rho v \\ \rho uv \\ \rho v^2 + p \\ v(E + p) \end{pmatrix} = 0, \quad (6)$$

where ρ , $\mathbf{V} = (u, v)$ and p are the density, velocity and pressure respectively while the total energy per unit volume E is given by

$$E = \rho \left(\frac{1}{2} \mathbf{V}^2 + e \right), \quad \mathbf{V}^2 = u_1^2 + u_2^2, \quad e = \frac{p}{\rho(\gamma - 1)},$$

where e is the specific internal energy and γ the ratio of specific heats.

The reconstruction is classically done on the primitive variables ρ, u, v, p and we use the same CellPD and EdgePD for all variables in a cell. In other words, the two notions are linked to cells and edges and not affected by the number of variables. Furthermore steps 5 and 6 of the previous MOOD algorithm are substituted with the following stages.

5. **Density DMP test.** The DMP criterion is checked on the density

$$\min_{j \in \mathcal{V}(i)} (\rho_i^n, \rho_j^n) \leq \rho_i^* \leq \max_{j \in \mathcal{V}(i)} (\rho_i^n, \rho_j^n). \quad (7)$$

If ρ_i^* does not satisfy (7) the **CellPD** is decremented, $\mathbf{d}_i := \max(0, \mathbf{d}_i - 1)$.

6. **Pressure positivity test.** The pressure positivity is checked and if $p_i^* \leq 0$ and \mathbf{d}_i has not been altered by step 5 then the **CellPD** is decremented, $\mathbf{d}_i := \max(0, \mathbf{d}_i - 1)$.

7. **Stopping criterion.** If for all $i \in \mathcal{E}_{el}$, \mathbf{d}_i has not been altered by steps 5 and 6 then the iterative procedure stops with $u_h^{n+1} = u_h^*$ else go to step 2.

4 Numerical results

Scalar case

The reader should refer to [5] for a complete study on the effective convergence rate. In this paper, we restrict the presentation to two representative tests. We first deal with the classical Solid Body Rotation (see [5] for details) test case for the advection problem.

We plot in Fig. 3 isolines top views of the solution obtained with the MOOD method applied to different polynomial degrees and meshes. Method name, triangles number and computational times are embedded in each figure. Time is given in relative time units (r.t.u) where MOOD-P1 is taken as reference with 100 r.t.u.

First solutions obtained on the 5190 cells mesh clearly show that the MOOD method is able to handle high-order polynomials with a great improvement of solutions while enforcing a strict DMP. Then the bottom line of Fig. 3 proves that it is more interesting to use polynomials of high degree compared to refining the mesh.

Finally the computational cost increase is mainly due to the reconstruction step. However since profiles are not smooth the DMP is often violated and the iterative procedure cost more than in the smooth case. For example a sixth-order unlimited version of the scheme costs 586 r.t.u., thus the iterative procedure costs about a third of the total time of the MOOD-P5 computation. Nevertheless this cost remains competitive and could be improved by a finer implementation.

Euler equations case

For the system case, a Rayleigh-Taylor Instability for the Euler equations with gravity is considered. The reader should refer to [8] for complete de-

scription of the test case.

The pattern of the unstructured symmetric triangular mesh used and the density solutions on a 28800 triangles mesh for MOOD-P1, MOOD-P3 and MOOD-P5 are plotted in Fig. 4. Computational time is given in r.t.u.

As for the scalar case the MOOD method is plainly able to improve the solution through the use of high-order polynomial reconstructions. From a computational cost point of view, computational times given in Fig. 4 prove that the MOOD iterative procedure is effective since the time raise from a degree to a bigger one is mainly due to the reconstruction cost itself.

References

1. R. Abgrall, On Essentially Non-oscillatory Schemes on Unstructured Meshes: Analysis and Implementation, *J. Comput. Phys.* **114** 45–58 (1994)
2. T. J. Barth, Numerical methods for conservation laws on structured and unstructured meshes, VKI March 2003 Lectures Series
3. T. J. Barth, D. C. Jespersen, The design and application of upwind schemes on unstructured meshes, AIAA Report 89-0366 (1989)
4. T. Buffard, S. Clain, Monoslope and Multislope MUSCL Methods for unstructured meshes, *J. Comput. Phys.* **229** 3745-3776 (2010)
5. S. Clain, S. Diot, R. Loubère A high-order finite volume method for systems of conservation laws Multi-dimensional Optimal Order Detection (MOOD), Submitted to *J. Comput. Phys.*
6. C. F. Ollivier-Gooch, Quasi-ENO Schemes for Unstructured Meshes Based on Unlimited Data-Dependent Least-Squares Reconstruction, *J. Comput. Phys.* **133** 6–17 (1997)
7. J. S. Park, S.-H. Yoon, C. Kim, Multi-dimensional limiting process for hyperbolic conservation laws on unstructured grids, *J. Comput. Phys.* **229** 788–812 (2010)
8. J. Shi, Y-T Zhang, C-W Shu, Resolution of high order WENO schemes for complicated flow structures, *J. Comput. Phys.* **186** 690–696 (2003)
9. W. R. Wolf , J. L. F. Azevedo, High-order ENO and WENO schemes for unstructured grids, *International Journal for Numerical Methods in Fluids*, **55** Issue 10 917–943 (2007)

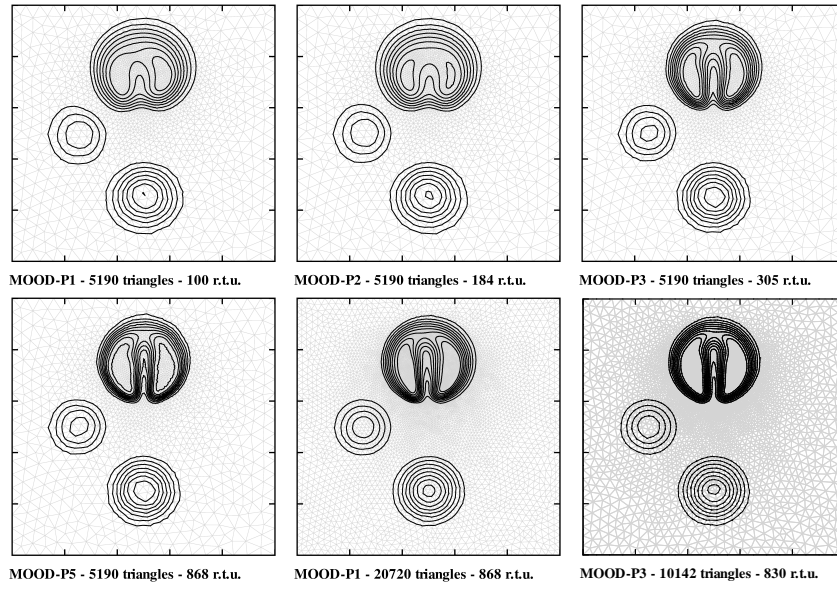


Fig. 3 Solid Body Rotation — 10 isolines from 0 to 1. Time is given in r.t.u.

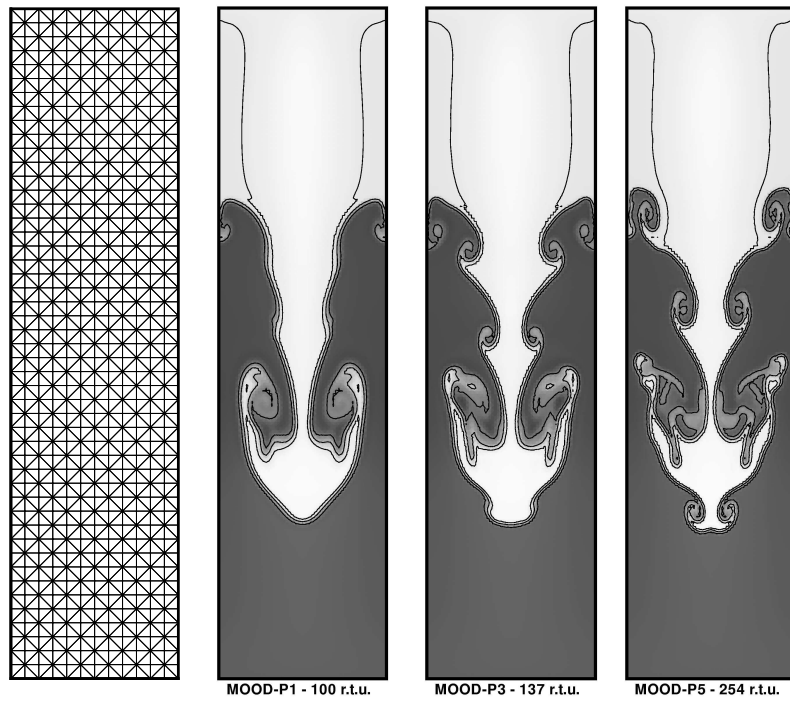


Fig. 4 Rayleigh-Taylor Instability — 5 isolines from 0.8 (dark) to 2.3 (light).